

# Analysis of contact forces in the walking gait of a quadruped robot

Diego Palma and Renzo Solórzano

Universidad de Ingeniería y Tecnología – UTEC, Lima, Perú

**Abstract**—Four foot trajectories for quadruped robots were compared and analyzed in this paper with a Solo12 robot. The trajectories were: sinusoidal, cycloidal, simple up and down function, and the Bezier Curves. Each of these trajectories were simulated in three different environments: a flat one, an uneven one and one with a wedge. Force contact sensors were used in the Pybullet dynamic simulator in order to obtain a physical measure to compare and represent these trajectories. The results were showed in boxplots, where the median and outliers were obtained; tables of the mean and the standard deviation of each trajectory; and plots of the contact forces during a period of time. Finally, after the comparisons were made, some trajectories stood out for determined environments.

**Index Terms**—foot trajectories, quadruped robot, contact forces, Pybullet

## I. INTRODUCTION

Research in quadruped robots has received a lot of attention because of its greater dexterity in harsh scenarios, which allows them to perform a wide range of activities such as logistics, construction, rescue, search, and detection [1], [2]. Although innovative mechanical structures and cutting-edge hardware provide legged robots with agility, their complete deployment is hampered by a wide range of potential factors that can destabilize robots in such conditions [3]. One of these factors is the trajectory followed by the robot's foot during a walking gait and the smoothness of its performance, because this kind of quadruped gait is related to the stability of the robot and it is used to enhance its robustness [4].

In the case of a walking gait, the leg movement mainly consists of two phases: a stance phase and a swing phase [5]. The stance phase is a moment when the legs are stressed, so the most contact forces occur in this phase. On the other hand, the swing phase is when the movement of the foot is performed, so the contact force is zero in this part. In this context, the smoothness of the foot trajectory is related to the contact forces on their feet. For this reason most of these quadruped robots include a contact sensor on their feet, besides it is useful for many torque-control strategies [6], energy efficiency analysis [7] and monitoring the walking gait of the robot [4]. Moreover, it is important to keep reaction forces in low values because high magnitudes could reduce the lifetime of the actuators and deteriorate the structure of the robot.

Therefore, in this paper we analyze the contact forces generated by four different foot trajectories: sinusoidal, cycloid, a simple up and down function, and the Bezier curves. From this, we will determine which trajectory produce lower contact

forces with a simple PD controller. Also, we will discuss which of them have a better performance during the walking gait in different environments.

The present paper is organized as follows. In section 2 is presented the methodology used for generating the foot trajectories, the robot used to implement it and the environments where the walk gait is tested. Section 3 shows the obtained results and the discussion of which of the trajectories have a better performance. Finally some conclusions are shown.

## II. METHODOLOGY

In the present section we describe the robot used to implement the foot trajectories and the software to perform simulations. Then, we show the four trajectories analyzed in this paper. Finally, we present the three environments created to further analysis of the contact forces in the walking gait.

### A. An open quadruped robot: Solo 12

The Solo robot [8] is a fully open-source legged robot with 12 degree-of-freedom (dof). This robot presents a modular force-controlled leg architecture for dynamic legged robot research. Moreover, it possess a light-weight foot contact sensor that can accurately detect contact forces in all directions and is suited for robots that are subjected to harsh impacts. Therefore, this robot fits our purposes in a future implementation.

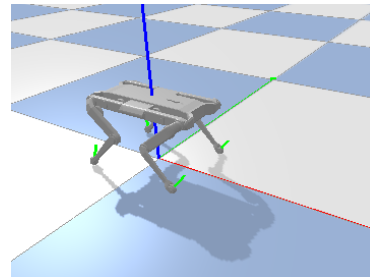


Fig. 1: Solo 12 in Pybullet environment

To simulate foot trajectories and measure contact forces we use Pybullet [9], a real-time collision detection and multi-physics simulation commonly used in robotics. This Python module adds robotics capabilities to the Bullet Physics Engine. Bullet solves the equations of motion in generalized coordinates for articulated rigid bodies while also meeting physical constraints such as contact, joint restrictions, and actuator models. After that, a semi-implicit approach is used to numerically integrate the system's state across time [10]. Due to all its features and continuous improvement, this software

is suitable for this project. In figure 1 the Solo 12 is shown in the Pybullet environment.

### B. Foot trajectories

1) *Sinusoidal trajectory*: This is one of the most common trajectories for bipedal and quadruped robots [11]–[13]. The created algorithm commands the foot trajectory to follow a sine wave, shown in figure 2a. The equations that represent a walking gait as a sine function are:

$$x(t) = x_0 - A_x \cos(2\pi t/T + \theta_x) \quad (1)$$

$$z(t) = \begin{cases} z_0 + A_z \sin(2\pi t/T + \theta_z) & t \leq T/2 \\ 0 & t > T/2 \end{cases} \quad (2)$$

where  $A_x$  and  $A_z$  are the amplitudes for each function,  $x_0$  and  $z_0$  are position of reference for the foot to oscillate around,  $\theta_x$  and  $\theta_z$  are the phases of the sinusoidal waves and  $T$  is the period. Usually  $z_0$  is a zero value so that the foot starts the trajectory from the ground.  $x_0$  takes the value of the position of the foot when the robot is not walking so the foot desired position is oscillating around this value, generates the walking and maintains the stability of the robot.

2) *Cycloidal trajectory*: The cycloidal trajectory has widely used for locomotion of a Quadruped Robot [14]–[17]. This trajectory is described by the following equations:

$$x(t) = x_0 + A_x \left( \frac{t}{T} - \frac{\sin(2\pi t/T)}{2\pi} \right) \quad t = [0, T] \quad (3)$$

$$z(t) = \begin{cases} z_0 + A_z \left( \frac{t}{T} - \frac{\sin(4\pi t/T)}{4\pi} \right) & t = [0, \frac{T}{4}] \\ z_0 + A_z - A_z \left( \frac{t}{T} - \frac{\sin(4\pi t/T)}{4\pi} \right) & t = [\frac{T}{4}, \frac{T}{2}] \\ 0 & t = [\frac{T}{2}, T] \end{cases} \quad (4)$$

where  $A_x$  and  $A_z$  are the amplitudes for each function,  $T$  is the period,  $t$  is the step time, and  $x_0$  and  $z_0$  is similar than in the sinusoidal trajectory. In figure 2b is shown the described trajectory.

3) *Simple up and down trajectory*: This simple trajectory is implemented because of its simplicity and fast implementation. The reason to implement it is verify if more sophisticated trajectories has a better performance than this trajectory or not. This trajectory is described by the following equations:

$$x(t) = \begin{cases} x_0 + \frac{4tA_x}{T} - A_x & t = [0, \frac{T}{2}] \\ x_0 - \frac{4tA_x}{T} + 3A_x & t = [\frac{T}{2}, T] \end{cases} \quad (5)$$

$$z(t) = \begin{cases} z_0 + 4A_z \frac{t}{T} & t = [0, \frac{T}{4}] \\ z_0 + 2A_z - 4A_z \frac{t}{T} & t = [\frac{T}{4}, \frac{T}{2}] \\ 0 & t = [\frac{T}{2}, T] \end{cases} \quad (6)$$

where  $A_x$  and  $A_z$  are the amplitudes for each function,  $T$  is the period,  $t$  is the step time, and  $x_0$  and  $z_0$  is similar than in the sinusoidal trajectory. In figure 2c is shown the described trajectory.

4) *Bezier Curves*: This is a smooth curve defined by a number of determined points. This method of foot trajectory is used in many robots such as MIT Cheetahs [18]. The swing trajectory is determined by the next equation:

$$B(t) = \sum_{i=0}^n \binom{n}{i} P_i (1-t)^{n-i} t^i \quad (7)$$

where  $P_i$  are called fitting point and are the ones that control the Bezier curve [5]. This kind of curve has some properties. For instance, a double coincidence in the fitting points determines a zero-velocity point and a triple coincidence determines a zero-acceleration point. Also, [5] proposes to use 12 fitting points and the properties mentioned to obtain a smooth curve as it can be seen in figure 2d.

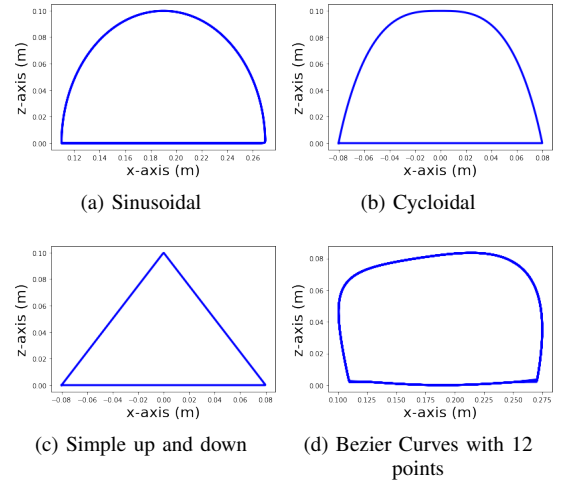


Fig. 2: Foot's Trajectory

### C. Simulation Environments

The four previous foot trajectories were tested and analyzed in three different environments: a flat ground, an uneven terrain and a wedge with  $10^\circ$  of inclination. The first one is the ideal environment without inclination or obstacle in middle of the way (Fig. 3a). The second one tries to simulate a rocky terrain using numerous blocks in varied positions and heights so the robot feet are in constant change of ground reference (Fig. 3b). Finally the third environment represents a ground with a inclination angle of  $10^\circ$ . This last test has the objective to analyse the stability of the robot while it descends from the top (Fig. 3c). It is important to mention that for each environment we performed 10 tests with each foot trajectory so more reliable results can be obtained.

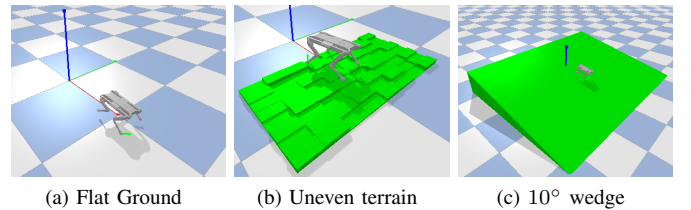


Fig. 3: Simulation environments

### III. RESULTS AND DISCUSSION

In this section we show the most relevant plots of the tests performed for each environment. Firstly, we show a plot of the mean contact force in each foot to know if this metric is constant along all the tests. Also, we made a table indicating the mean with its standard deviation. Secondly, since the mean is altered by high contact forces, we did a boxplot to show the median contact force. Finally, we made a time plot to know the behavior of the contact forces during the walking gait. To have a more readable plot the zero forces were removed, which means only the stance phase of the walking gait is shown.

#### A. Flat environment

Figure 4 shows the mean contact force in z-axis for each foot trajectory along 10 tests. We can see that the simple trajectory mean forces are one of the highest in the front feet but the lowest in the rear feet. Additionally, the sinusoidal trajectory presents, in general, a better performance than the other ones since it has the second lowest mean forces for each foot. It is important to mention that all the trajectories, except the cycloidal one, show similar values along all the tests.

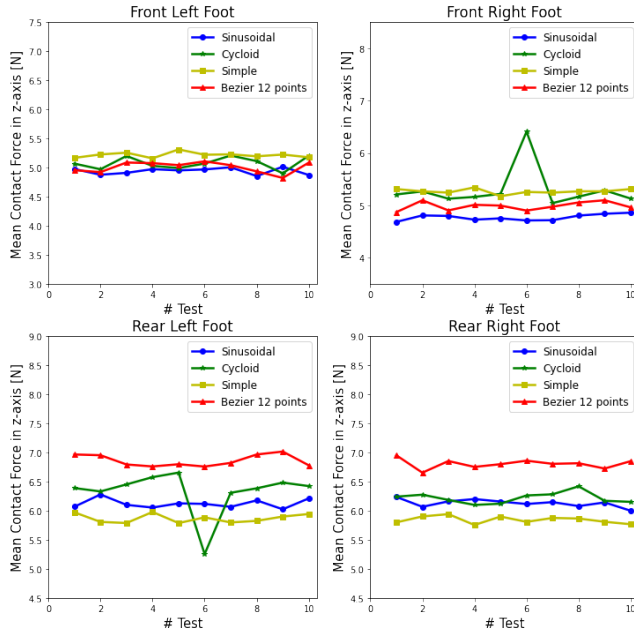


Fig. 4: Mean contact force of each trajectory in a flat environment

In Table I the mean contact forces are shown with its standard deviation (std). As we can see, all the trajectories has a high *std*, which indicates that mean is being affected by many contact forces peaks during the walking gait.

TABLE I: Media and Standard Deviation of forces in a flat environment

Foot\Trajectory	Sinusoidal	Bezier12	Cycloid	Simple
FR	4.773 $\pm$ 6.473	5.023 $\pm$ 6.588	5.186 $\pm$ 8.306	5.271 $\pm$ 6.568
FL	4.943 $\pm$ 6.616	4.946 $\pm$ 6.471	5.08 $\pm$ 7.771	5.219 $\pm$ 6.433
BR	6.131 $\pm$ 6.960	6.716 $\pm$ 7.971	6.221 $\pm$ 7.012	5.842 $\pm$ 6.043
BL	6.120 $\pm$ 6.957	6.929 $\pm$ 8.064	6.440 $\pm$ 7.216	5.867 $\pm$ 5.993

Then, in figure 5 we can see the median contact force in a boxplot. The highest contact forces are shown as outliers as well. From this, the Bezier curve presents the highest values in the back feet, meanwhile the cycloidal trajectory presents them in the front feet. Furthermore, the Bezier curve has the lowest median contact forces in all the feet.

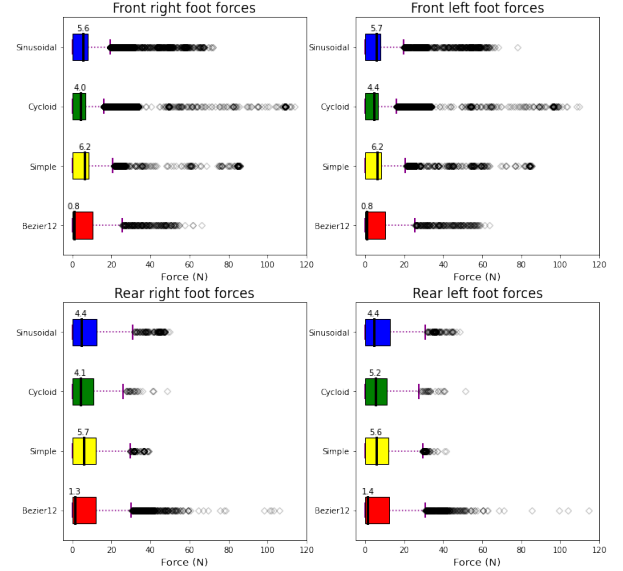


Fig. 5: Boxplot of each trajectory in a flat environment

Regarding the behavior of the contact force during the walking gait, in figure 6 the contact forces over the time (for a random test) in each foot are shown. The forces appears first in the front right and the rear left legs, indicating that the robot starts walking with the left front foot. It can be seen that all the trajectories has a smooth and constant behaviour in the front legs, but only the Bezier curve has not force peaks. In the rear legs, only the Bezier curve and the simple trajectory have an smooth behaviour, as they do not have high rate of variation in their values. However, the Bezier curve has the highest forces, as shown in figure 5.

#### B. Uneven environment

For this environment, the simple trajectory has the lowest mean forces for each test. On the other hand, the trajectories with the highest mean forces in each foot, are the Bezier curve ones, as it can be seen in figure 7. In this case, only the simple trajectory presents a constant value of the mean contact force. This is important because indicates that the forces tend to be uniform during all the tests. Likewise, in Table II the mean contact force and the standard deviation for all the tests are shown. The values of the latter are as high as in the flat environment.

As in the flat environment, the median of the contact forces is plotted on the boxplot of figure 8. As we can see, the Bezier curve presents the highest forces in each foot, that is why the Bezier curves has the highest values in figure 7 and the highest standard deviation as well in the previous table. In addition,

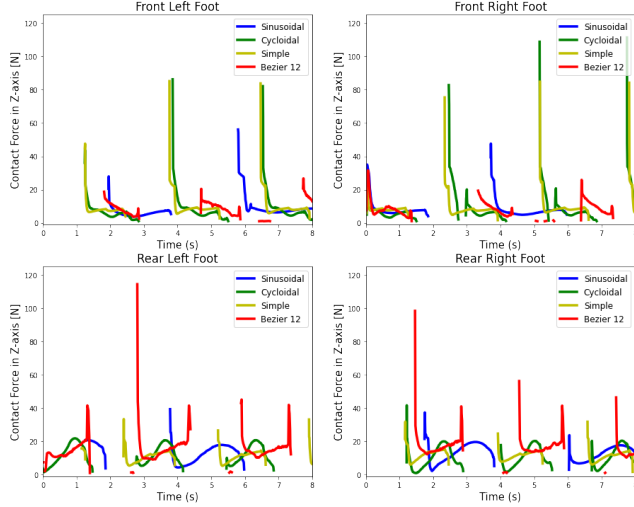


Fig. 6: Contact forces during the walking gait in the flat environment

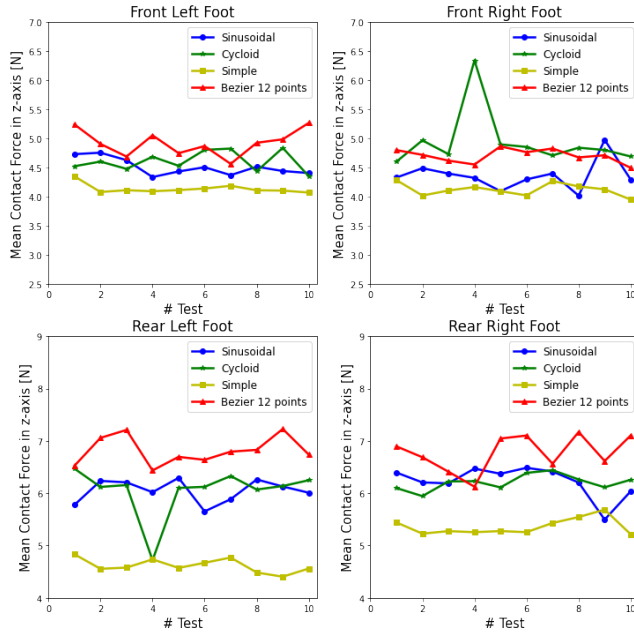


Fig. 7: Mean contact force of each trajectory in an uneven environment

TABLE II: Media and Standard Deviation of forces in an uneven environment

Foot\Trajectory	Sinusoidal	Bezier12	Cycloid	Simple
FR	$4.369 \pm 6.705$	$4.756 \pm 10.075$	$4.785 \pm 7.704$	$4.119 \pm 5.884$
FL	$4.511 \pm 6.939$	$4.913 \pm 9.786$	$4.607 \pm 7.813$	$4.137 \pm 5.858$
BR	$6.235 \pm 7.408$	$6.728 \pm 9.219$	$6.204 \pm 7.559$	$5.364 \pm 6.525$
BL	$6.048 \pm 7.344$	$6.809 \pm 9.378$	$6.212 \pm 7.361$	$4.612 \pm 6.159$

the sinusoidal trajectory has the lowest median force in this environment and also it has few force peaks over all the tests.

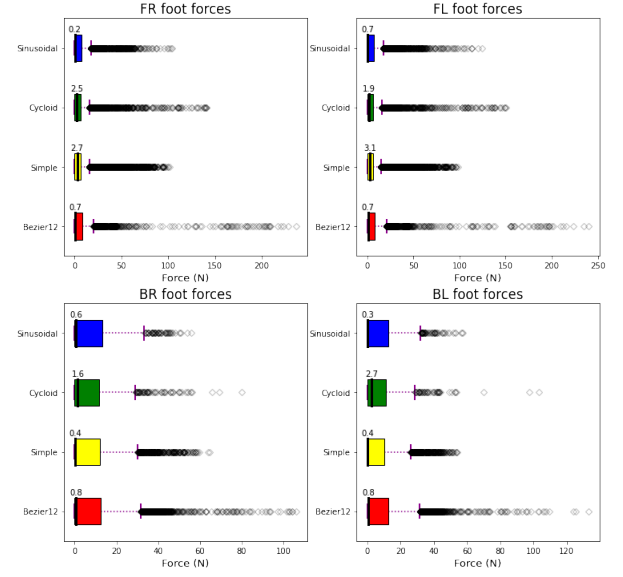


Fig. 8: Boxplot of each trajectory in an uneven environment

In figure 9 the behavior of the contact force on an uneven terrain are shown. In this environment the robot starts walking with the left foot as well. Likewise, all the trajectories has a similar behaviour and presents similar peaks, except for the Bezier curves which are the highest. In this case it is important to note that high peaks occur when the foot has to move from a higher brick to a lower one because there is a higher lineal momentum (impulse).

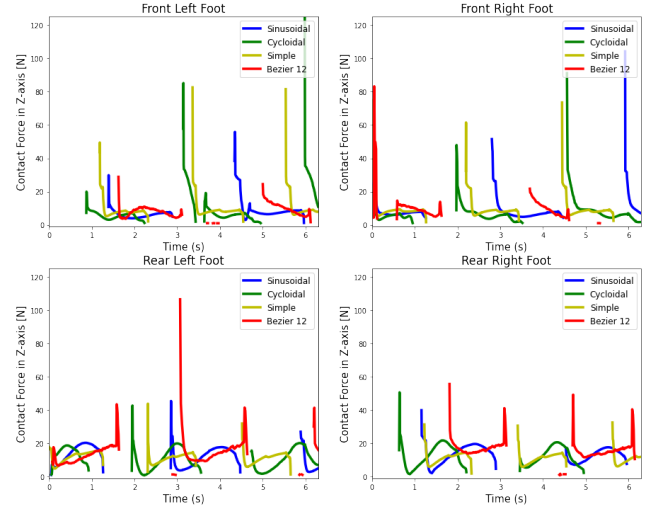


Fig. 9: Contact forces during the walking gait in an uneven environment

### C. Environment with a wedge

Lastly the result of the mean forces for the descent of the wedge is shown in figure 10. The simple trajectory exhibits the best performance as its behaviour seems constant in all the tests, it has the lowest forces in the rear feet and the second

lowest in the front feet. Despite the fact that the sinusoidal trajectory has the lowest mean forces in the front feet.

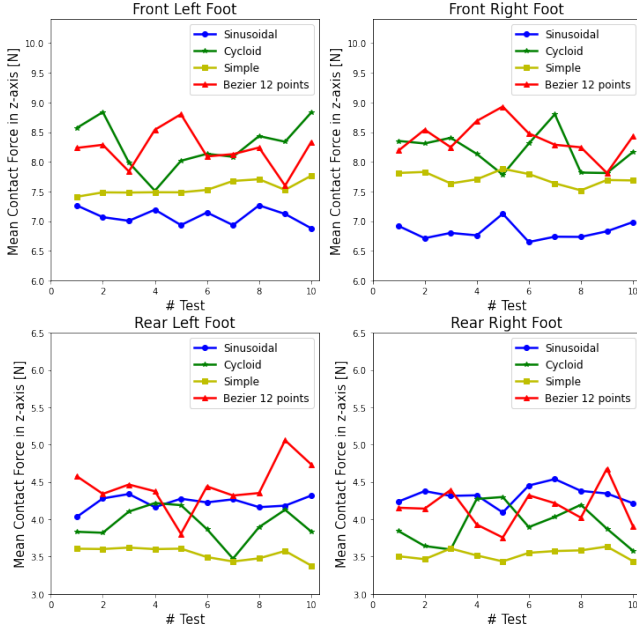


Fig. 10: Mean contact force of each trajectory in a wedge

In Table III the values for the media and standard deviation of all the tests for this environment are shown. From this table and the following plots, it is possible to notice that the front feet in all trajectories have the highest forces as they support the majority of the robot weight during the descent. The Bezier curves present the highest standard deviation due to this trajectory have the most elevated peaks, which can be seen in figure 12.

TABLE III: Media and Standard Deviation of forces in a wedge

Foot \ Trajectory	Sinusoidal	Bezier12	Cycloid	Simple
FR	6.828 ± 8.868	8.186 ± 18.662	8.184 ± 10.395	7.074 ± 8.535
FL	7.081 ± 8.956	7.946 ± 18.529	8.275 ± 10.528	6.947 ± 8.513
BR	4.326 ± 5.333	3.979 ± 6.483	3.922 ± 5.551	3.863 ± 4.932
BL	4.224 ± 5.333	4.361 ± 6.545	3.939 ± 5.503	3.812 ± 4.861

The boxplot for this environment are shown in figure 11. In spite of the Bezier curve having the highest peaks, it has the lowest median in the front feet. This means that in the majority of the walking gait, the forces maintain themselves in this range but at the first contact with the ground the forces increase to elevated values and then they return. In the rear feet, the cycloid trajectory presents the lowest median as well as the lowest peaks during its path.

Finally the plot of the forces behaviour during a period of time is presented in figure 12. In this front feet, it can be seen the elevated peaks of the Bezier curve trajectory mentioned previously and the constant behaviour after these peaks. The lowest peaks were made by the sinusoidal trajectory. Additionally, all the trajectories show smooth and constant behaviours after their peaks. On the other hand, in the rear

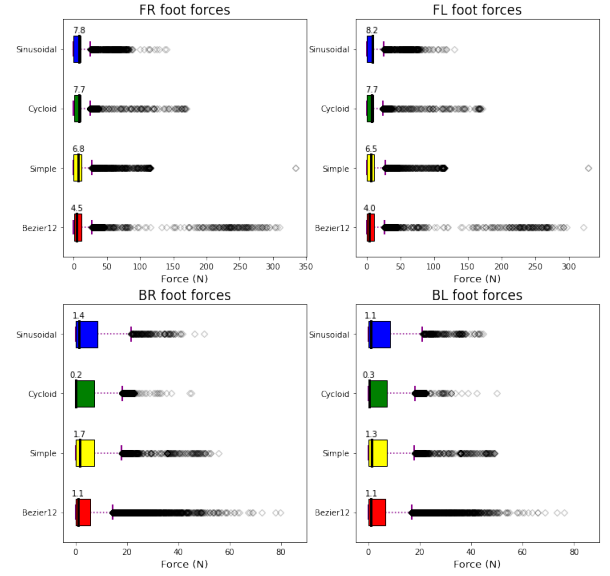


Fig. 11: Boxplot of each trajectory in a wedge

feet, the trajectory which has the lowest peaks and smoothest curves seems to be the simple up and down trajectory, while the sinusoidal, Bezier and cycloidal curves present the second peak they have presented in all the environments.

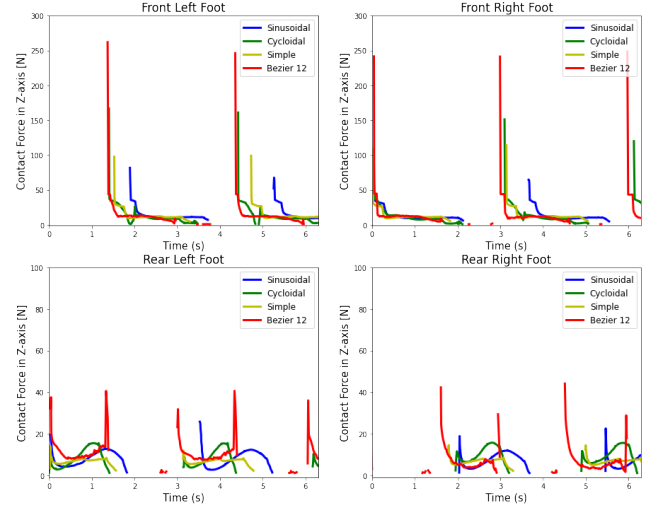


Fig. 12: Contact forces during the walking gait in an environment with a  $10^\circ$  wedge

#### IV. CONCLUSIONS

In this paper was analyzed the contact forces generated by four foot trajectories during the walking gait of the Solo 12 robot in three different and common environments. In the flat environment, the Bezier curves generated the lowest median contact force which indicate this trajectory allows the robot to have the lowest contact forces during the walking gait. However, there are some instances where the contact force is higher, so it is recommended to saturate the measurement of these forces, at least in the front legs. On the other hand, the simple up and down trajectory is more suitable in the



uneven terrain because of its behaviour and it keeps contact forces low during most of the walk, as well. In this case, to pass the environment as fast as possible, it is important to have an amplitude greater than the height of the bricks. In none of the tests did the robot fall down, but when tested with lower amplitudes it was slower than normal. Regarding the environment with a wedge, the simple and the Bezier curve trajectories would be recommendable options; however, the simple one would be chosen again for this environment. Despite the fact that the Bezier curve presented the lowest median in the front feet, it presents enormous peaks, which can negatively affect the actuators and the structure of the robot. Also it fell in one of the tests while the robot using the simple trajectory kept walking in every test.

Another metric that could be important to take in account is how naturally the robot walks. However, deciding this can be subjective. From the point of view of the authors, Bezier curves make the robot walk more naturally, while the most unnatural walk occurs with the simple trajectory.

## REFERENCES

- [1] P. Biswal and P. K. Mohanty, "Development of quadruped walking robots: A review," *Ain Shams Engineering Journal*, vol. 12, pp. 2017–2031, jun 2021.
- [2] C. Semini and P.-B. Wieber, *Legged Robots*, p. 1–8. Springer Berlin Heidelberg, 2020.
- [3] H. Sun, T. Fu, Y. Ling, and C. He, "Adaptive quadruped balance control for dynamic environments using maximum-entropy reinforcement learning," *Sensors*, vol. 21, no. 17, 2021.
- [4] X. Li, W. Wang, and J. Yi, "Foot contact force of walk gait for a quadruped robot," in *2016 IEEE International Conference on Mechatronics and Automation*, pp. 659–664, 2016.
- [5] X. Zeng, S. Zhang, H. Zhang, X. Li, H. Zhou, and Y. Fu, "Leg trajectory planning for quadruped robots with high-speed trot gait," *Applied Sciences*, vol. 9, no. 7, p. 1508, 2019.
- [6] Y. H. Lee, Y. H. Lee, H. Lee, H. Kang, J. H. Lee, L. T. Phan, S. Jin, Y. B. Kim, D.-Y. Seok, and S. Y. e. a. Lee, "Development of a quadruped robot system with torque-controllable modular actuator unit," *IEEE Transactions on Industrial Electronics*, vol. 68, no. 8, pp. 7263–7273, 2021.
- [7] J. Lei, F. Wang, H. Yu, T. Wang, and P. Yuan, "Energy efficiency analysis of quadruped robot with trot gait and combined cycloid foot trajectory," *Chinese Journal of Mechanical Engineering*, vol. 27, pp. 138–145, 01 2014.
- [8] F. Grimmering, A. Meduri, M. Khadiv, J. Viereck, M. Wüthrich, M. Naveau, V. Berenz, S. Heim, F. Widmaier, T. Flayols, J. Fiene, A. Badri-Spröwitz, and L. Righetti, "An open torque-controlled modular robot architecture for legged locomotion research," *IEEE Robotics and Automation Letters*, vol. 5, no. 2, pp. 3650–3657, 2020.
- [9] E. Coumans and Y. Bai, "Pybullet, a python module for physics simulation for games, robotics and machine learning," <http://pybullet.org>, 2016–2021.
- [10] J. Tan, T. Zhang, E. Coumans, A. Iscen, Y. Bai, D. Hafner, S. Bohez, and V. Vanhoucke, "Sim-to-real: Learning agile locomotion for quadruped robots," 2018.
- [11] J.-K. Han, *Bipedal walking for a full size humanoid robot utilizing sinusoidal feet trajectories and its energy consumption*. PhD thesis, Virginia Tech, 2012.
- [12] Y. Sakakibara, K. Kan, Y. Hosoda, M. Hattori, and M. Fujie, "Low-impact foot trajectory for a quadruped walking machine," *Advanced robotics*, vol. 7, no. 4, pp. 343–360, 1992.
- [13] N. Kau, A. Schultz, N. Ferrante, and P. Slade, "Stanford doggo: An open-source, quasi-direct-drive quadruped," in *2019 International Conference on Robotics and Automation (ICRA)*, pp. 6309–6315, 2019.
- [14] Y. Zeng, J. Li, S. X. Yang, and E. Ren, "A bio-inspired control strategy for locomotion of a quadruped robot," *Applied Sciences*, vol. 8, no. 1, 2018.
- [15] J. Li, D. Cong, and Z. Yang, "A method of foot trajectory generation for quadruped robots in swing phase to optimize the joint torque," in *IOP Conference Series: Materials Science and Engineering*, vol. 491, p. 012002, IOP Publishing, 2019.
- [16] Y. Lu, X. Q. Zhao, Z. X. Zhang, J. Z. Shang, and Z. R. Luo, "Research on improved cycloid foot trajectory of quadruped robot," in *Advances in Mechatronics and Control Engineering*, vol. 278 of *Applied Mechanics and Materials*, pp. 576–581, Trans Tech Publications Ltd, 3 2013.
- [17] L. Wang, "Strategy of foot trajectory generation for hydraulic quadruped robots gait planning," *Journal of Mechanical Engineering*, vol. 49, p. 39, 2013.
- [18] D. J. Hyun, S. Seok, J. Lee, and S. Kim, "High speed trot-running: Implementation of a hierarchical controller using proprioceptive impedance control on the mit cheetah," *The International Journal of Robotics Research*, vol. 33, no. 11, pp. 1417–1445, 2014.